

Direct amine-functionalisation of γ -Fe₂O₃ nanoparticles

Cite this: *Dalton Trans.*, 2014, **43**, 2948

V. Rocher,^a J. Manerova,^b M. Kinnear,^a D. J. Evans^a and M. G. Francesconi^{*a}

Received 29th August 2013,
Accepted 25th November 2013

DOI: 10.1039/c3dt52386a

www.rsc.org/dalton

A novel and simple preparation of amine-modified γ -Fe₂O₃ nanoparticles is described. The presence of amine groups on the surface, instead of hydroxyl groups, will allow conjugation of biologically active molecules to the iron oxide nanoparticles without the need for a size increasing silica shell. Furthermore, the outer amine-layer increases the temperature of the γ -Fe₂O₃ to α -Fe₂O₃ structural transition in a similar way to previously reported cationic substitutions. This may suggest the formation of an oxide-nitride outer layer. Re-dispersion of the amine-modified γ -Fe₂O₃ nanoparticles led to the preparation of stable ferrofluids.

Introduction

A simple route was used to prepare a ferrofluid from nanoparticles directly functionalised with amine groups. Ferrofluids are generally made of nanoparticles of iron oxide dispersed into a liquid medium to form a stable colloidal solution.¹ The magnetic moment carried by the nanoparticles makes these dispersions responsive to external magnetic fields² opening up a number of interesting potential applications.^{3–5} In order to obtain stable ferrofluids, aggregation between the magnetic nanoparticles must be avoided and, generally, this is achieved by functionalisation, *e.g.* surface binding of molecules to create steric hindrance,⁶ either directly on the nanoparticles' surface or through additional silica shells. By careful choice of the molecule, the properties of ferrofluids can be tailored towards different applications. Direct functionalisation can be achieved by bonding molecules to hydroxyl groups present on the surface of the nanoparticles, the advantage being that the size of the nanoparticles is maintained as there is no need for an additional silica shell. The requirement for amine-functionalised nanoparticles is dictated by certain types of molecules, for example complex biologically active molecules, which will bind to the nanoparticles *via* an amide bond.⁷

Ferrofluids are most commonly dispersions of either γ -Fe₂O₃ (maghemite) or Fe₃O₄ (magnetite) nanoparticles or a mixture of both. The two structures of γ -Fe₂O₃ and Fe₃O₄ are

both based on a FCC lattice of O^{2–} anions, with Fe₃O₄ containing both Fe²⁺ and Fe³⁺ cations, and γ -Fe₂O₃ Fe³⁺ cations and cation vacancies to maintain charge neutrality.^{8–10} Under thermal treatment cubic, ferromagnetic maghemite transforms irreversibly into the rhombohedral antiferromagnetic hematite (α -Fe₂O₃).¹¹ This structural transition is being investigated with the aim of increasing the temperature limit of stability of the maghemite phase to maintain its magnetic properties and widen the applicability of γ -Fe₂O₃. For example, γ -Fe₂O₃ shows high sensitivity and selectivity in sensors for hydrocarbon gases, without the need for a noble metal.¹² Cation doping of γ -Fe₂O₃ nanoparticles seems to be the most effective way to increase the temperature of the γ -Fe₂O₃/ α -Fe₂O₃ transition, but very little has been reported on transition temperature variations caused by functionalisation. Here we report that reacting γ -Fe₂O₃ nanoparticles with NH₃ (g) at 200 °C for 2–4 hours leads to direct functionalisation of the nanoparticles with amine groups and increases the temperature of the structural transition from γ -Fe₂O₃ (maghemite) to α -Fe₂O₃ (hematite) up to 550 °C. This suggests the possibility of formation of an outer layer of iron oxide-nitride.

Experimental

Preparation of nanoparticles of γ -Fe₂O₃

Iron oxide nanoparticles were prepared *via* a sol-gel process.¹³ A solution of iron(II) and iron(III) chlorides in water was reacted with ammonium hydroxide to form magnetite (Fe₃O₄) nanoparticles. After washing with acetone and ether, the nanoparticles were re-dispersed in nitric acid. Reaction with iron(III) nitrate at boiling point oxidised the nanoparticles to maghemite (γ -Fe₂O₃).

^aDepartment of Chemistry, University of Hull, Cottingham Road, Hull, HU6 7RX, UK.
E-mail: m.g.francesconi@hull.ac.uk; Fax: +44 (0)1482 46 6410;
Tel: +44 (0)1482 46 5409

^bChemical and Biological Engineering Department, The University of Sheffield, Sir Robert Hadfield Building, Mappin Street, Sheffield, S1 3JD, UK.
E-mail: j.manerova@sheffield.ac.uk; Fax: +44 (0)114 222 7501;
Tel: +44 (0)114 222 7500



Amination of $\gamma\text{-Fe}_2\text{O}_3$ nanoparticles with NH_3 (g)

Dried nanoparticles of $\gamma\text{-Fe}_2\text{O}_3$ were placed into a small ceramic reaction boat, which was placed at the centre of the tube in a tube furnace. The flow rate of ammonia gas was 4.0 L h^{-1} and excess was removed by an HCl scrubber. The temperature was raised to 200°C at 5°C min^{-1} and maintained between 1 and 2 hours. At the end of the reaction, the tube was flushed with nitrogen to remove unreacted ammonia and the product was transferred to a glove box for storage under argon.

Ferrofluids were prepared by dispersion of $\gamma\text{-Fe}_2\text{O}_3$ nanoparticles and amine-modified $\gamma\text{-Fe}_2\text{O}_3$ nanoparticles. A sample of approximately 100 mg was added to 2 mL of aqueous solution of HNO_3 ($\text{pH} = 2$). This suspension was then subjected to 30 minutes of ultrasonic radiation to break the larger aggregates. The resulting colloidal dispersions were left to rest for 24 hours to test their stability.

Powder X-ray diffraction was carried out using a Siemens D5000 diffractometer using the $\text{Cu K}\alpha$ radiation. Data were recorded from $2\theta = 10^\circ$ to $2\theta = 110^\circ$ over 72 hours, with a step size of 0.02° .

Thermogravimetric analyses were carried out using a Mettler TGA/DSC 1 Starsystem. 10–15 mg of nanoparticles were placed in an alumina pan and heated at a constant rate ($30^\circ\text{C min}^{-1}$) to 900°C under air, with the weight pattern and heat flow recorded as functions of the temperature.

The nitrogen content of the N-doped samples was measured using a CE Instruments 1108 CHN analyzer and results were expressed as weight percentages.

Nitrogen adsorption isotherms were recorded on a Micromeritics Tristar 3000. Size distribution was calculated from these data using the BJH model.

To demonstrate qualitatively the presence of surface amine groups, portions of ferrofluids formed with $\gamma\text{-Fe}_2\text{O}_3$ nanoparticles and $\gamma\text{-Fe}_2\text{O}_3$ nanoparticles reacted with ammonia were reacted for 1 h with a solution of fluorescamine (4'-phenylspiro[2-benzofuran-3,2'-furan]-1,3'-dione) in acetone (1 mg in 5 mL). The nanoparticles were then removed by filtration and the presence of fluorophors was revealed by examining the solutions under UV light.

Mössbauer spectra were recorded in zero magnetic field at 80 K on an ES-Technology MS-105 Mössbauer spectrometer with a $900 \text{ MBq } ^{57}\text{Co}$ source in a rhodium matrix at ambient temperature. Spectra were referenced against a $25 \mu\text{m}$ iron foil at 298 K and spectrum parameters were obtained by fitting with Lorentzian curves. Samples were ground with boron nitride before mounting in the sample holder.

Results and discussion

The size of the nanoparticles, calculated from nitrogen adsorption data, shows sizes distributed between 4.5 nm and 6.0 nm for initial $\gamma\text{-Fe}_2\text{O}_3$ particles and between 5.5 nm and 7.0 nm for $\gamma\text{-Fe}_2\text{O}_3$ reacted with ammonia; the reaction with ammonia caused only a limited increase of the size of the $\gamma\text{-Fe}_2\text{O}_3$

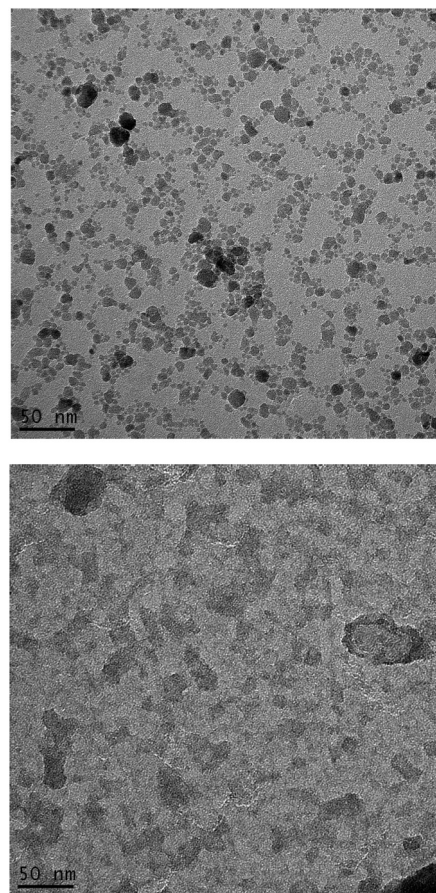


Fig. 1 TEM images of $\gamma\text{-Fe}_2\text{O}_3$ nanoparticles (top) and $\gamma\text{-Fe}_2\text{O}_3$ nanoparticles reacted with ammonia at 200°C for 2 hours (bottom).

nanoparticles, although aggregation took place after reaction with ammonia gas, as shown by TEM images (Fig. 1).

Stable colloidal suspensions (ferrofluids) were obtained by sonication in de-ionised water using both $\gamma\text{-Fe}_2\text{O}_3$ nanoparticles and $\gamma\text{-Fe}_2\text{O}_3$ nanoparticles reacted with ammonia.

Powder X-ray diffraction (PXRD) of $\gamma\text{-Fe}_2\text{O}_3$ nanoparticles and $\gamma\text{-Fe}_2\text{O}_3$ nanoparticles reacted with NH_3 (g) for 1 and 2 hours at 200°C are shown in Fig. 2. The PXRD pattern of the $\gamma\text{-Fe}_2\text{O}_3$ nanoparticles shows the $\gamma\text{-Fe}_2\text{O}_3$ single phase. The percentage of $\gamma\text{-Fe}_2\text{O}_3$ versus Fe_3O_4 was calculated *via* a peak deconvolution method to be 98.66%.¹⁴ The $\gamma\text{-Fe}_2\text{O}_3$ structure is maintained after ammoniation at 200°C up to 2 hours and no formation of impurities can be detected. The unit cell parameters of all three compounds were refined from the general model for spinel-type structures, *i.e.* a face-centred cubic unit cell (space group $Fd\bar{3}m$, number 227). No substantial difference was observed between the unit cell parameters of the three samples analysed ($a = 8.349(1) \text{ \AA}$ for $\gamma\text{-Fe}_2\text{O}_3$; $a = 8.337(2) \text{ \AA}$ for $\gamma\text{-Fe}_2\text{O}_3 + \text{NH}_3$ (g) for 1 hour; $a = 8.335(1) \text{ \AA}$ for $\gamma\text{-Fe}_2\text{O}_3 + \text{NH}_3$ (g) for 2 hours).^{17,18} The findings of the refinements are in agreement with those reported by Petkov *et al.*¹⁹ The nitrogen content (weight%) was determined by elemental analysis to be 0.05% and 0.24% for nanoparticles reacted with ammonia for 1 and 2 hours, respectively.



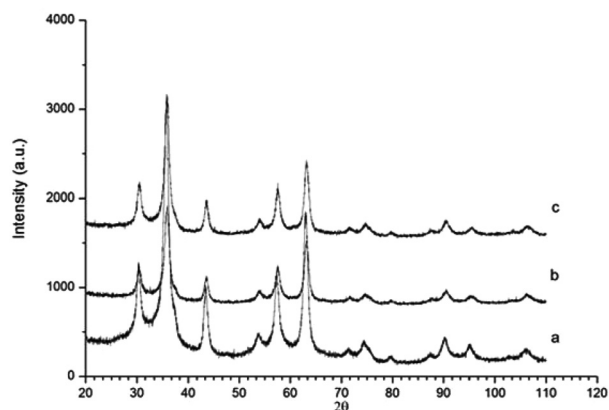


Fig. 2 PXRD diffractograms of γ -Fe₂O₃ nanoparticles before and after reaction with NH₃ for different times. (a) Initial γ -Fe₂O₃ nanoparticles; (b) nanoparticles reacted for 1 hour; (c) nanoparticles reacted for 2 hours.

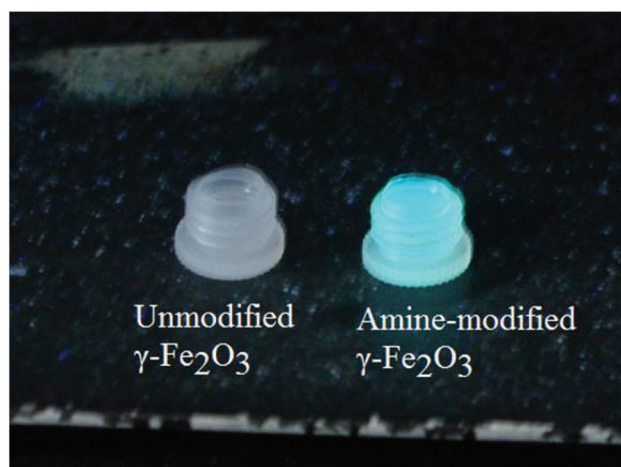


Fig. 3 Fluorescamine test showing fluorescence only on reaction with amine-modified γ -Fe₂O₃ nanoparticles.

Reactions of both γ -Fe₂O₃ nanoparticles and ammoniated γ -Fe₂O₃ nanoparticles with fluorescamine were carried out to investigate qualitatively the presence of amine groups on the surface of the ammoniated γ -Fe₂O₃ nanoparticles.¹⁵ Fluorescamine does not fluoresce itself but, after reaction with amine functional groups, forms a highly fluorescent fluorophor. Furthermore, fluorescamine is specific for primary amines as it does not react with secondary amines and forms a non-fluorescent adduct with ammonia.¹⁶ The formation of fluorophors was observed only for the nanoparticles that had been reacted with ammonia (Fig. 3), indicating that primary amines have replaced a portion of the hydroxide groups on the surface of the γ -Fe₂O₃ nanoparticles. Further evidence of amine-functionalisation is the pH of the ferrofluid suspensions, which was consistently between 11 and 12.

Reactions between Fe₃O₄, α -Fe₂O₃ and Fe with NH₃ and/or NH₃/H₂ at temperatures between 350 and 900 °C have resulted in a variety of iron nitrides.^{20–23} Tessier *et al.* and Kikkawa

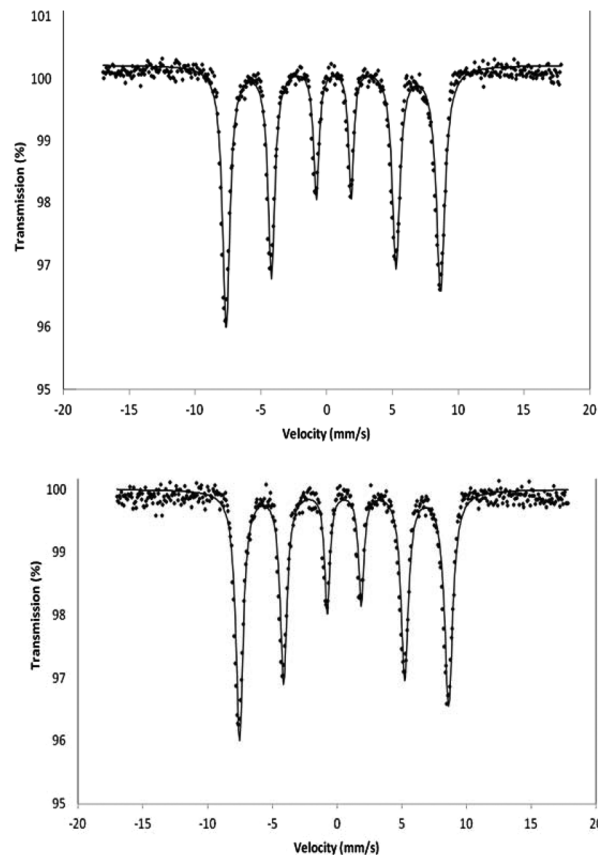


Fig. 4 Mössbauer spectrum of γ -Fe₂O₃ (top) and γ -Fe₂O₃ after 2 hours treatment with ammonia (bottom) recorded in the solid state at 80 K in zero magnetic field.

et al. reported the formation of Fe₁₆N₂ via a ‘soft chemistry’ route, *i.e.* by using low temperatures and long times, reacting α -Fe₂O₃ with ammonia for 10 days at 110 °C²⁴ or for 100 hours at 130 °C, after reduction of α -Fe₂O₃ to α -Fe.²⁵ In our work, low temperature and short reaction times have led to breakage of bonds between the surface of the nanoparticles and –OH groups and to their replacement with –NH₂ groups, as well as the probable formation of a thin oxide–nitride layer. The fact that PXRD showed no structural changes and/or secondary phases, the small nitrogen content detected *via* elemental analyses, and the results from the fluorescamine experiment eliminate the formation of an iron nitride and support direct functionalisation of γ -Fe₂O₃ nanoparticles with amine groups.

Zero-field Mössbauer spectra for γ -Fe₂O₃ and γ -Fe₂O₃ nanoparticles after ammoniation were recorded (Fig. 4). The spectrum for each sample is indistinguishable from the other and confirms that the γ -Fe₂O₃ structure is maintained on ammoniation. There is no evidence for magnetite or significant amounts of impurity being present. Only one hyperfine pattern is observed as expected in zero field and the spectra correspond to those previously reported for γ -Fe₂O₃.^{26,27}

The TGA and heat flow diagram for γ -Fe₂O₃ nanoparticles heated in air (Fig. 5, top) shows an initial sharp weight loss due to physisorbed and chemisorbed moisture and hydroxyl



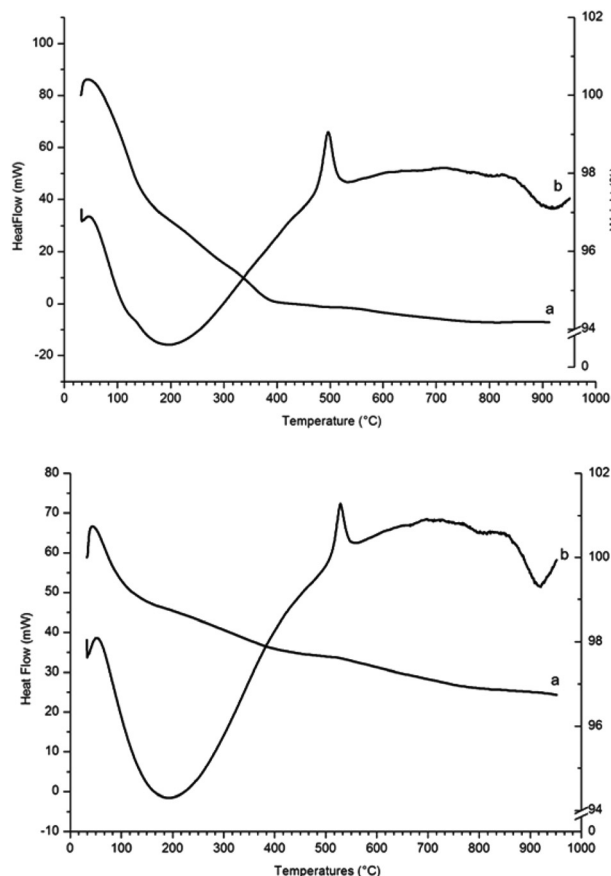


Fig. 5 TGA and DSC analysis in air of γ -Fe₂O₃ nanoparticles (top) and γ -Fe₂O₃ nanoparticles reacted with NH₃ (g) for 2 hours at 200 °C (bottom) ((a) weight of the sample as percentage of initial weight; (b) heat flow).

groups. The heat flow shows a large exothermic peak at 495 °C corresponding to transformation of γ -Fe₂O₃ into α -Fe₂O₃, in agreement with the transition temperature reported by E. Darezereshki, who focussed on γ -Fe₂O₃ nanoparticles of similar size (13 and 19 nm).²⁸ The residue samples from TGA analyses were analysed by PXRD and the patterns showed only diffraction peaks belonging to the α -Fe₂O₃ phase.

The TGA and heat flow diagrams for γ -Fe₂O₃ nanoparticles reacted with NH₃ (g) for 2 hours at 200 °C (Fig. 5, bottom) show a weight loss between room temperature and 400 °C that is probably due to loss of amino groups from the surface of the nanoparticles. The heat flow shows that the exothermic peak corresponding to transformation of γ -Fe₂O₃ into α -Fe₂O₃ has shifted from 495 °C to 550 °C.

A comparison of the exothermic heat flow peaks indicating the γ -Fe₂O₃ to α -Fe₂O₃ transition temperature, for all three samples, is shown in Fig. 6. The transition temperature increases from 495 °C for the γ -Fe₂O₃ nanoparticles to 526 °C for γ -Fe₂O₃ nanoparticles reacted with NH₃ (g) for 1 hour, and to 550 °C for the γ -Fe₂O₃ nanoparticles reacted with NH₃ (g) for 2 hours.

The maghemite-hematite structural transition has been discussed in a recent review on polymorphous transformation

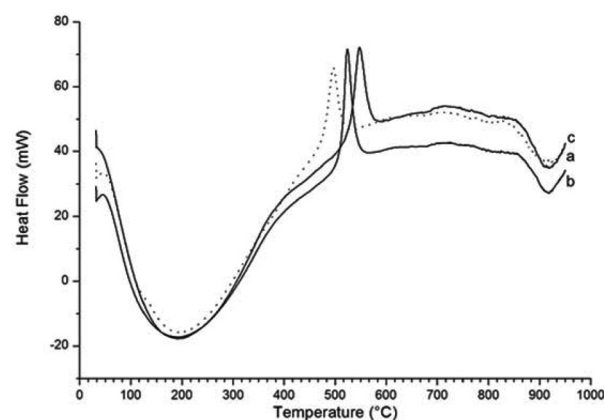


Fig. 6 Comparison of the heat flow diagrams for (a) γ -Fe₂O₃ nanoparticles (dotted line) and (b) γ -Fe₂O₃ nanoparticles reacted for 1 hour and (c) for 2 hours.

of nanometric iron(III) oxides.²⁹ The maghemite to hematite phase transition was studied using differential thermal analysis³⁰ and *in situ* real time X-ray diffraction.^{31,32} Different transition temperatures have been reported for nanoparticles of maghemite (200–500 °C) and for micro-sized particles (500 and 600 °C)³³ and cation doping has been found to be a useful tool to enhance the transition temperature. Doping of amorphous Fe₂O₃ with 8.5% Mn³⁺ led to γ -Fe₂O₃ nanoparticles after heating for 3 hours at 500 °C³⁴ and Zn²⁺ doping enhances the phase transformation temperature by *circa* 100 °C.³⁵ DSC studies under air of Zn_xFe_{3-x}O₄ ($x = 0, 0.2, 0.4$, and 0.6) solid solution showed that the γ -Fe₂O₃ to α -Fe₂O₃ phase transition temperature increases with increase in zinc content.³⁶ A study on Fe_{3-x}Co_xO₄ solid solutions showed that for $x = 0.1$ the temperature of the γ -Fe₂O₃ to α -Fe₂O₃ transition was increased by about 100 °C.³⁷ γ -Fe₂O₃ nanoparticles doped with La³⁺ showed no sign of phase transition to α -Fe₂O₃ after 8 hours at 400 °C.³⁸

Here, we show that the γ -Fe₂O₃ to α -Fe₂O₃ transition temperature is enhanced up to 550 °C as a consequence of the reaction of γ -Fe₂O₃ nanoparticles with ammonia. PXRD data show no changes in the patterns indicating no formation of nitrides, but it is likely that a thin layer of oxide-nitride is formed on the surface of the γ -Fe₂O₃ nanoparticles. It has been reported that the α/γ structural transition occurs as the size of the particles increases; hence an O/N layer is likely to decompose in air as the temperature increases (TGA carried out in air), hence delaying the α/γ structural transition. Whether the presence of primary amines on the surface of γ -Fe₂O₃ nanoparticles has any influence on the γ -Fe₂O₃ to α -Fe₂O₃ transition temperature is difficult to assess. Functionalisation of γ -Fe₂O₃ nanoparticles with palmitic acid was reported to shift the γ -Fe₂O₃ to α -Fe₂O₃ transition temperature up to 400 °C.³⁹ Two sets of γ -Fe₂O₃ nanoparticles were functionalised with PMMA (poly-methyl methacrylate) and with caprylate respectively and their γ versus α phase stability compared.⁴⁰ The γ -Fe₂O₃ to α -Fe₂O₃ transition occurred at 400 °C for the caprylate-capped γ -Fe₂O₃ nanoparticles and at 500 °C for the γ -Fe₂O₃/PMMA composite



γ -Fe₂O₃. It was argued that the outer molecular layer creates a barrier, which slows down the aggregation of the nanoparticles and consequent structural transition. However, in our case the coating of the nanoparticles alone may not be very effective in hindering particle aggregation as -NH₂ groups provide an outer layer of comparable thickness to the -OH layers.

Conclusion

In summary, we prepared γ -Fe₂O₃ nanoparticles and reacted them with NH₃ (g) at 200 °C for 1 and 2 hours. We obtained directly amine-functionalised γ -Fe₂O₃ nanoparticles, *i.e.* γ -Fe₂O₃ nanoparticles with NH₂ groups substituting -OH surface groups. Normally, a silica shell is needed to prepare amine-functionalised γ -Fe₂O₃ nanoparticles; however, this additional layer contributes to increasing the size of the nanoparticles, a disadvantage for medical applications. The amine-functionalised nanoparticles did not show any sizeable increase in their diameter, were re-dispersed in water to form stable ferrofluids and showed, therefore, suitability for reactions with application-controlling molecules. TGA coupled with heat flow measurements showed that the presence of the amine layer and, probably, of an oxide-nitride surface layer also enhances the γ -Fe₂O₃ to α -Fe₂O₃ transition temperature up to 550 °C, comparable to previously reported cation modifications.

Notes and references

- 1 R. Massart, *IEEE Trans. Magn.*, 1981, **17**(2), 1247.
- 2 J.-C. Bacri, R. Perzynski, D. Salin, V. Cabuil and R. Massart, *J. Magn. Magn. Mater.*, 1986, **62**(1), 36.
- 3 K. Raj, B. Moskowitz and R. Casciari, *J. Magn. Magn. Mater.*, 1995, **149**(1–2), 174.
- 4 I. Sharifi, H. Shokrollahi and S. Amiri, *J. Magn. Magn. Mater.*, 2012, **324**(6), 903.
- 5 R. Banerjee, Y. Katsenovich, L. Lagos, M. McIntosh, X. Zhang and C.-Z. Li, *Curr. Med. Chem.*, 2010, **17**(27), 3120.
- 6 E. Amstad, M. Textor and E. Reimhult, *Nanoscale*, 2011, **3**, 2819.
- 7 T. Georgelin, V. Maurice, B. Malezieux, J.-M. Siaugue and V. Cabuil, *J. Nanopart. Res.*, 2010, **12**(2), 675.
- 8 J. E. Jorgensen, L. Mosegaard, L. E. Thomsen, T. R. Jensen and J. C. Hanson, *J. Solid State Chem.*, 2007, **180**, 180.
- 9 C. Greaves, *J. Solid State Chem.*, 1983, **49**, 325.
- 10 T. J. Bastow, A. Trinchin, M. R. Hill, R. Harris and T. H. Muster, *J. Magn. Magn. Mater.*, 2009, **321**(17), 2677.
- 11 R. M. Cornel and U. Schwertmann, *The Iron Oxides. Structure, Properties, Reactions and Uses*, 2003.
- 12 D.-D. Lee and D.-H. Choi, *Sens. Actuators, B*, 1990, **1**, 231.
- 13 N. Fauconnier, A. Bée, J. Roger and J. N. Pons, *J. Mol. Liq.*, 1999, **83**(1–3), 233.
- 14 W. Kim, C.-Y. Suh, S.-W. Cho, K.-M. Roh, H. Kwon, K. Song and I.-J. Shon, *Talanta*, 2012, **94**, 348.
- 15 O. S. Wolfbeis, M. Hof, R. Hutterer and V. Fidler, *Fluorescence Spectroscopy in Biology*, Springer, Berlin, 2005.
- 16 R. Kellener, F. Lottspeich and H. E. Meer, *Microcharacterization of Proteins*, 2nd edn, 1999.
- 17 A. C. Larson and R. B. Von Dreele, General Structure Analysis System (GSAS), *Los Alamos National Laboratory Report LAUR 86-748*, 2004.
- 18 B. H. Toby, EXPGUI, *J. Appl. Crystallogr.*, 2001, **34**, 210.
- 19 V. Petkov, P. D. Cozzoli, R. Buonsanti, R. Cingolani and Y. Ren, *J. Am. Chem. Soc.*, 2009, **131**, 14264–14266.
- 20 X. L. Wu, W. Zhong, N. J. Tang, H. Y. Jiang, W. Liu and Y. W. Du, *J. Alloys Compd.*, 2004, **385**, 294.
- 21 S. Kurian and N. S. Gajbhiye, *J. Nanopart. Res.*, 2010, **12**, 1197.
- 22 S. Kurian and N. S. Gajbhiye, *Chem. Phys. Lett.*, 2010, **493**, 299.
- 23 W. Arabczyk, J. Zamlynny and D. Moszynski, *Pol. J. Chem. Technol.*, 2010, **12**, 38.
- 24 F. Tessier, *Solid State Sci.*, 2000, **2**, 457.
- 25 S. Kikkawa, K. Kubota and T. Takeda, *J. Alloys Compd.*, 2008, **449**, 7.
- 26 N. N. Greenwood and T. C. Gibb, *Mössbauer Spectroscopy*, 1971, ch. 10, pp. 240–258.
- 27 Y. R. Uhm, W. W. Kim and C. K. Rhee, *Phys. Status Solidi A*, 2004, **201**, 1934.
- 28 E. Darezereshki, *Mater. Lett.*, 2011, **65**, 642.
- 29 L. Machala, J. Tuek and R. Zbořil, *Chem. Mater.*, 2011, **23**, 3255.
- 30 X. Ye, D. Lin, Z. Jiao and L. Zhang, *J. Phys. D: Appl. Phys.*, 1998, **31**, 2739.
- 31 T. Belina, N. Millot, N. Bovet and M. Gailhanou, *J. Solid State Chem.*, 2007, **180**, 2377.
- 32 G. Schimanke and M. Martin, *Solid State Ionics*, 2000, **136**, 1235.
- 33 G. Ennas, A. Mei, A. Musinu, G. Piccaluga, G. Pinna and S. Solinas, *J. Mater. Res.*, 1999, **14**(4), 1570.
- 34 J. Lai, K. V. P. M. Shafi, K. Loos, A. Ulman, Y. Lee, T. Vogt and C. Estournes, *J. Am. Chem. Soc.*, 2003, **125**, 11470.
- 35 S. Deka and P. A. Joy, *J. Mater. Chem.*, 2007, **17**, 453.
- 36 S. S. Pati and J. Philip, *J. Appl. Phys.*, 2013, **113**(4), 044314/1.
- 37 S. S. Pati, S. Gopinath, G. Panneerselvam, M. P. Antony and J. Philip, *J. Appl. Phys.*, 2012, **112**(5), 054320/1.
- 38 H. Wang, N. Hua, Y. Du and P. Yang, *Huaxue Yanjiu Yu Yingyong*, 2005, **17**(3), 369.
- 39 R. Zboril, A. Bakandritsos, M. Mashlan, V. Tzitzios, P. Dallas, C. Trapalis and D. Petridis, *Nanotechnology*, 2008, **19**, 095602.
- 40 T. Ninjbadgar, S. Yamamoto and M. Takano, *Solid State Sci.*, 2005, **7**, 33.

